

A SEVEN-YEAR PHOTOMETRIC STUDY OF THREE ACTIVE GALACTIC NUCLEI

SARAH A. MARHEINE¹

Department of Physics, Lawrence University, P.O. Box 599, Appleton, WI 54912

AND

KENNETH S. RUMSTAY

Department of Physics, Astronomy, and Geosciences, Valdosta State University, 1500 N. Patterson St., Valdosta, GA 31698

ABSTRACT

In order to further our understanding of the structure of the broad emission-line regions of AGNs, we have analyzed the Seyfert galaxies 3C-120, Mrk 79, and Mrk 704 using relative and absolute photometric methods. This will hopefully lead to an ability to use reverberation mapping to estimate the geometry and mass of the central regions of these objects. We also provide an overview of the current model of an AGN and a brief description of the technique of reverberation mapping.

Subject headings: galaxies: active, photometry, individual (3C-120, Mrk 79, Mrk 704) — techniques: photometric

1. INTRODUCTION

This section is intended to provide a cursory introduction to the anatomy of AGNs and the technique of reverberation mapping. It is far from exhaustive, and much more in-depth discussions of these topics may be found in the works included in the references.

1.1. AGNs and the Broad Line Region

In 1943, Carl Seyfert noticed the similarities in the emission line spectra of a handful of galaxies. A few of these objects were identified as radio sources in 1955, and interest in Seyfert's galaxies was renewed. Other radio surveys discovered the objects known as quasars, and these together with the Seyfert Galaxies and other luminous X-ray sources fall under the category of active galaxies, or AGNs when referring specifically to the nucleus. This central region is typically much brighter than the disk of the galaxy itself; in general, little besides the nucleus can be resolved.

The currently accepted model of a typical AGN begins with a central black hole. The masses of these objects can vary greatly, but are typically in the range of 10^6 to 10^9 solar masses (Peterson 1997). These black holes are the "engines" of the objects, providing the gravitational energy that powers all the other processes.

Surrounding the black hole are an accretion disk of infalling matter, a broad-line region, and a narrow-line region (Peterson 2004). The broad-line region is occupied by gas clouds of relatively high density; these are responsible for the broad (10^3 to 10^4 km/sec) permitted lines observed in Seyfert 1 spectra. At a much greater distance lies the narrow-line region. The lower-density clouds here produce the narrow (10^2 km/sec) forbidden lines observed in Seyfert spectra of all types. Figure 1 shows a schematic model of an AGN.

This study seeks to refine our knowledge of the BLR structures of three objects in particular: 3C-120, Mrk 79, and Mrk 704 (see also Table 1 and Figures 2, 3, and 4). We present optical data spanning the time period 2001 - 2007 for these objects.

1.2. Reverberation Mapping

Reverberation mapping is a technique commonly used to infer the size and geometry of the BLR. The first step is to track the variations in an AGN's luminosity, ideally over many years. To the light curves thus obtained, one can apply the *cross-correlation function*

$$L_{CCF}(\tau) = \int_{-\infty}^{\infty} L(t)C(t-\tau) dt,$$

where τ is the time delay that must occur when the light emitted by the source travels to and is reflected by the BLR clouds (Peterson 2004). Naturally, τ will depend on the characteristic size of the region and the particular shape of L_{CCF} will depend on its geometry.

In general, brightness variation with a longer period (that is, slower fluctuations) indicates a larger BLR and more massive central black hole. However, we have not yet begun this work, because we want a better idea of the shape of the light curves. This will require several more years' data.

2. OBSERVATIONS

The images used in this study were obtained using the SARA 0.9-m telescope at Kitt Peak National Observatory. We took short² CCD exposures, although some had to be extended to achieve a useful signal-to-noise ratio, which occasionally resulted in elliptical images. During the period 2001-2007 three different Apogee CCD cameras were used: AP7 (512×512 pixels, $6.2'$ -square image), U55 (770×1152 pixels, $8.7' \times 13.0'$ image), and U42 (1024×1024 pixels, $13.9'$ -square image). Images were obtained with Johnson *I*, *R*, *V*, and *B* filters on nearly every night of observation. A few images were not used in the survey because of very poor image quality or excessively large error in the calculated magnitudes (see Section 3.1).

3. PHOTOMETRY

In order to determine the magnitudes of our AGNs, we had to combine two different photometric techniques. The stars near 3C-120, Mrk 79, and Mrk 704 do not have published

¹ Southeastern Association for Research in Astronomy (SARA) NSF-REU Summer Intern
Electronic address: sarah.a.marheine@lawrence.edu

² approximately 60 to 360 seconds, depending on the object, filter, and conditions.

TABLE 1
POSITIONS AND REDSHIFTS FOR 3C-120, MRK 79, MRK 704^{1†}

Object	$\alpha(2000)$	$\delta(2000)$	z	I^{2*}	R^{2*}	V^{2*}	B^{2*}
3C-120	04 ^h 33 ^m 10.8 ^s	+05°21'19"	0.0331	150	150	220	300
uMrk 79	07 ^h 42 ^m 32.4 ^s	+49°48'41"	0.0219	150	180	240	360
Mrk 704	09 ^h 18 ^m 26.1 ^s	+16°18'20"	0.0299	60	60	80	120

^{1†}de Vaucouleurs et al. (1991)

^{2*} Typical CCD exposure times (seconds) for SARA telescope.

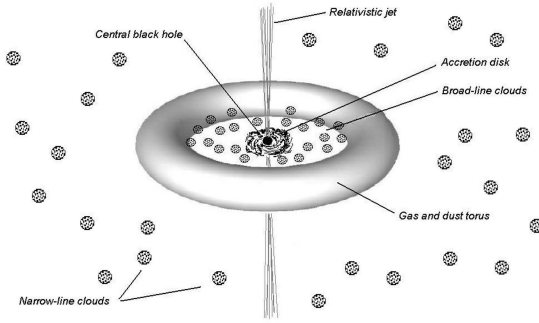


FIG. 1.— A generalized model of an AGN.

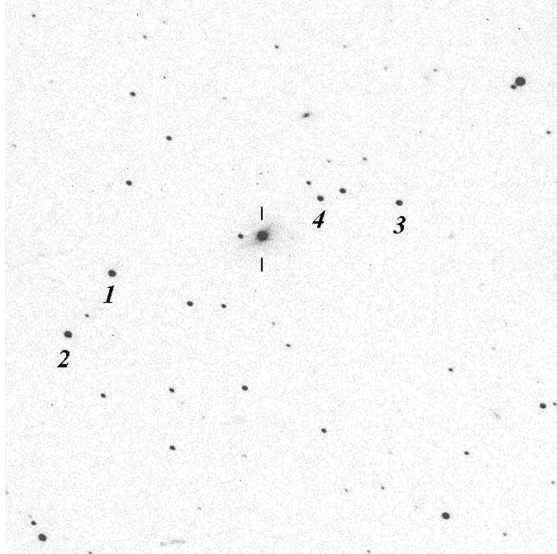


FIG. 2.— 3C-120 with comparison stars.

magnitudes in all the filters we require, so the first step in the process was to use an absolute photometric technique to determine values for those stars and verify that they were not variable. Once we obtained internally-consistent magnitudes, we were able to find AGN magnitudes and plot light curves.

The comparison stars we used are labeled in Figures 2 through 4.

3.1. Absolute Wide-Band Photometric Reduction

Determining absolute magnitudes of comparison stars using this method requires several images of different parts of the sky from the same night. At least two of these images must be of standard star fields with different airmasses, and

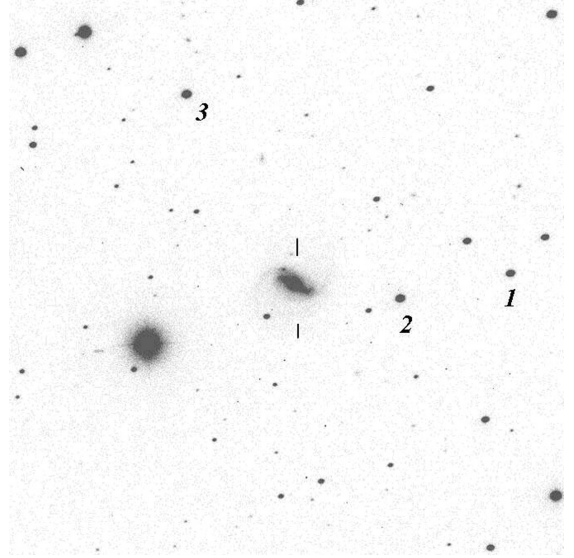


FIG. 3.— Mrk 79 with comparison stars.

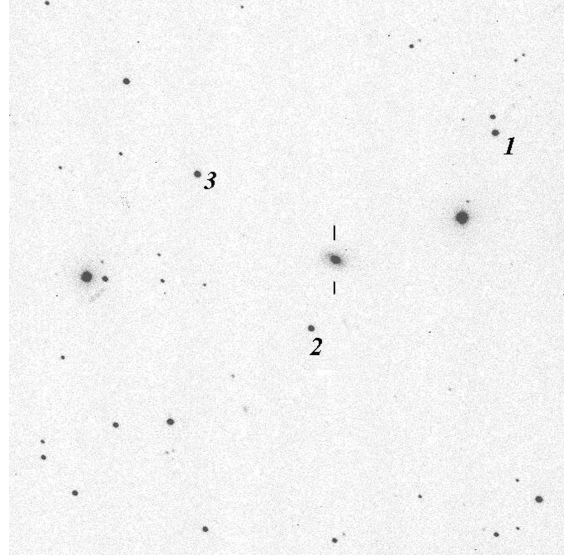


FIG. 4.— Mrk 704 with comparison stars.

one of the target field. The images used must also have been taken on a night with photometric conditions; that is, one with a completely clear sky. This is a somewhat rare occurrence at the SARA telescope, but appropriate conditions were finally encountered in March 2007, which allowed us to undertake this work.

The first step, once the images have been obtained, is to calculate the instrumental magnitudes and color indices using fluxes (S_{color}) obtained from the standard star fields:

$$\begin{aligned}
 v &= -2.5 \log S_V \\
 b-v &= -2.5 \log (S_B/S_V) \\
 v-r &= -2.5 \log (S_V/S_R) \\
 r-i &= -2.5 \log (S_R/S_I).
 \end{aligned}$$

(1)

Then we must correct for atmospheric extinction — the flux of each object is dimmed relative to the airmass for the field's position and the conditions of the night.

TABLE 2
ABSOLUTE PHOTOMETRIC COEFFICIENTS FOR 2007 MARCH 15.

First-order extinction	Second-order extinction	Transformation slope	Transformation intercept
$k'_V = 0.2112$	$k''_V = +0.0382$	$\epsilon = +0.0147$	$\zeta_V = +22.030$
$k'_{B-V} = 0.0562$	$k''_{B-V} = -0.1235$	$\mu = +1.0660$	$\zeta_{B-V} = -0.5819$
$k'_{V-R} = 0.1411$	$k''_{V-R} = -0.0197$	$\psi = +1.0270$	$\zeta_{V-R} = +0.0861$
$k'_{R-I} = 0.2091$	$k''_{R-I} = +0.0393$	$\phi = +1.1850$	$\zeta_{R-I} = +0.3835$

$$\begin{aligned}
v_o &= v - k'_V X - k''_V (b-v) X \\
(b-v)_o &= (b-v) - k'_{B-V} X - k''_{B-V} (b-v) X \\
(v-r)_o &= (v-r) - k'_{V-R} X - k''_{V-R} (b-v) X \\
(r-i)_o &= (r-i) - k'_{R-I} X - k''_{R-I} (b-v) X
\end{aligned}
\tag{2}$$

Finally, these magnitudes must be converted to the standard Johnson photometric system.

$$\begin{aligned}
V &= v_o + \epsilon (b-v)_o + \zeta_V \\
B-V &= \mu (b-v)_o + \zeta_{B-V} \\
V-R &= \psi (v-r)_o + \zeta_{V-R} \\
R-I &= \phi (r-i)_o + \zeta_{R-I}
\end{aligned}
\tag{3}$$

The coefficients in the above equations are specific to the night used. Our data are from 2007 March 15, and the numerical values of the coefficients are shown in Table 2.

After preliminary magnitudes have been calculated using this method, the values must be checked for internal consistency and to make sure that none of the stars we chose are variable. This is done by using the magnitudes obtained to do relative photometry in MIRA (see Section 3.2) — preferably on images from all available nights — then comparing the calculated magnitudes of the comparison stars to the adjusted ones from MIRA's output.

3.2. Relative Photometry with MIRA

MIRA is a commercially available image processing software package marketed by Axiom research. MIRA's built-in relative (or “aperture”) photometry process is relatively simple and will not be described in detail here.

Relative photometry is a process by which the magnitude of a target object can be determined by comparing its flux through an aperture with those of comparison objects in the same image. MIRA's output also recalculates values of the comparison stars themselves, which we used to determine the internal consistency of the calculated magnitudes. After those values were adjusted as necessary, we performed relative photometry on every image again to find AGN magnitudes and produce light curves (Tables 6–8; Figures 5–7; Section 4).

4. RESULTS

4.1. Comparison Star Magnitudes

The final comparison star magnitudes for our three AGNs (with error) are shown in Tables 3, 4, and 5. Stars 3 and 4 in 3C-120 should be applied with only half weight when used for relative photometry because of their dimness—the random uncertainty in their magnitudes is very high.

TABLE 3
3C-120 COMPARISON STAR MAGNITUDES.

Star	B	V	R	I
1	16.13 ± 0.07	15.36 ± 0.03	14.94 ± 0.03	14.53 ± 0.04
2	16.35 ± 0.07	15.44 ± 0.03	14.89 ± 0.03	14.41 ± 0.03
3	17.56 ± 0.17	16.60 ± 0.09	15.96 ± 0.07	15.39 ± 0.10
4	17.56 ± 0.13	16.61 ± 0.05	16.05 ± 0.05	15.54 ± 0.08

TABLE 4
MRK 79 COMPARISON STAR MAGNITUDES.

Star	B	V	R	I
1	15.63 ± 0.04	14.97 ± 0.02	14.54 ± 0.02	14.13 ± 0.04
2	14.94 ± 0.05	14.39 ± 0.01	13.99 ± 0.02	13.65 ± 0.02
3	15.22 ± 0.03	14.36 ± 0.01	13.81 ± 0.02	13.26 ± 0.02

TABLE 5
MRK 704 COMPARISON STAR MAGNITUDES.

Star	B	V	R	I
1	15.19 ± 0.04	14.64 ± 0.04	14.26 ± 0.03	13.93 ± 0.02
2	15.38 ± 0.04	14.90 ± 0.05	14.54 ± 0.02	14.23 ± 0.02
3	15.24 ± 0.03	14.59 ± 0.06	14.14 ± 0.02	13.68 ± 0.02

TABLE 6
MAGNITUDES OF 3C-120.

Julian date	I	R	V	B
2452156.91	13.682	14.108	14.544	15.203
2452207.78	13.704	14.135	14.646	15.360
2452234.79	13.694	14.006	14.630	15.159
2452240.74	13.647	13.999	14.694	15.182
2452331.68	13.650	14.199	14.685	15.398
2452529.96	13.475	13.833	14.360	14.963
2452576.77	13.456	13.818	14.262	14.887
2452597.78	13.372	13.765	14.178	...
2452624.73	13.364	13.818	14.271	14.846
2452662.65	13.396	13.799	14.350	14.899
2452669.68	13.466	13.807	14.363	14.915
2452899.02	13.708	14.086
2452949.80	13.564	13.936	14.432	14.959
2453052.66	13.585	13.907	14.485	...
2453395.69	13.597	14.057	14.501	15.192
2453437.64	13.650	14.092	14.652	15.321
2453626.91	13.367	13.797	14.319	14.964
2453670.79	13.483	13.838	14.369	14.971
2453766.65	13.673	14.089	14.608	15.269
2453997.92	13.674	14.085	14.599	15.267
2454029.85	13.625	14.044	14.611	15.299
2454055.85	13.692	14.123	14.774	15.419
2454083.69	13.866	14.227	14.792	15.577
2454116.70	13.778	14.190	14.746	15.540
2454153.66	13.601	14.030
2454174.64	13.581	13.944	14.463	15.194

4.2. Light Curves

With the adoption of comparison star magnitudes, we were able to determine B , V , R , and I magnitudes for 3C-120, Mrk 79, and Mrk 704 for each night of observation and to create light curves. These data are collected in Tables 6 through 8 and Figures 5 through 7.

TABLE 7
MAGNITUDES OF MRK 79.

Julian date	I	R	V	B
2451983.64	13.364	13.807	14.377	14.853
2452207.91	13.604	14.144	14.740	15.395
2452240.82	13.475	13.945	14.538	15.069
2452319.74	13.402	13.870	14.423	14.987
2452331.72	13.427	13.848	14.366	14.871
2452382.64	13.317	13.836	14.319	14.847
2452597.98	13.133	13.555	14.090	14.480
2452624.88	13.181	13.599	14.106	14.475
2452662.73	13.129	13.571	14.127	14.471
2452669.77	13.159	13.611	14.133	14.537
2452751.66	13.316	13.739	14.315	14.818
2452949.92	13.213	13.568	14.170	14.570
2453052.72	13.203	13.668	14.222	14.659
2453395.75	13.258	13.699	14.225	14.707
2453437.68	13.238	13.710	14.214	14.662
2453514.64	13.431	13.750	14.453	...
2453670.98	13.386	13.873	14.512	15.013
2453766.69	13.454	13.909	14.589	15.048
2453787.70	13.379	13.812	14.503	15.074
2454030.00	13.364	13.860	14.505	15.112
2454055.97	13.409	13.920	14.499	15.264
2454083.74	13.442	13.878	14.445	15.209
2454116.74	13.371	13.887	14.466	15.086
2454153.68	13.338	13.846	14.417	15.119
2454174.68	13.439	13.846	14.521	15.175
2454209.66	13.476	14.012	14.656	...
2454216.72	13.489	14.095	14.704	15.484

TABLE 8
MAGNITUDES OF MRK 79.

Julian date	I	R	V	B
2451983.67	13.413	13.938	14.461	14.972
2452240.86	13.559	14.054	14.564	15.040
2452319.77	13.490	13.906	14.423	14.850
2452382.70	13.424	13.834	14.349	14.780
2452412.66	13.403	13.849	14.362	14.731
2452598.02	13.494	13.963	14.499	14.995
2452624.98	13.473	13.942	14.474	14.958
2452669.82	13.453	13.937	14.481	14.940
2452751.71	13.478	13.943	14.531	14.999
2452950.04	13.489	13.916	14.522	...
2453052.74	13.605	14.102
2453071.81	13.622	14.138	14.672	15.223
2453395.79	13.577	...	14.567	14.927
2453437.72	13.498	13.998	14.563	15.058
2453465.73	13.565	14.098	14.626	15.130
2453671.01	13.622	14.097	14.653	15.166
2453766.71	13.607	14.140	14.621	15.159
2454030.02	13.512	13.938	14.487	15.008
2454055.98	13.469	13.863	14.374	14.916
2454116.78	13.360	13.832	14.356	14.820
2454153.71	13.370	13.845	14.372	14.851
2454174.71	13.370	13.863	14.325	14.929
2454209.71	13.391	13.841	14.387	14.971
2454216.70	13.436	13.882	14.427	14.867
2454248.66	13.412	13.950

The photometric uncertainties are typically 0.02 to 0.04 mag in *I*, *R*, and *V*, and 0.02 to 0.05 mag in *B*. In the plots, the error bars would be on the order of the size of the spot itself.

Some data points have been omitted because of excessive error. We feel this is justified because, on some occasions, the image quality was less than desirable.

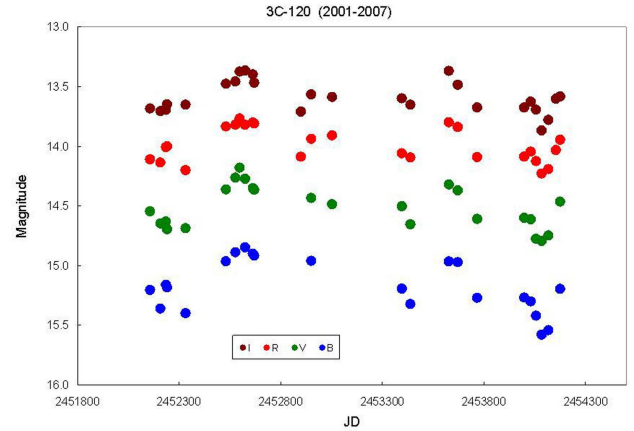


FIG. 5.— The light curves for 3C-120.

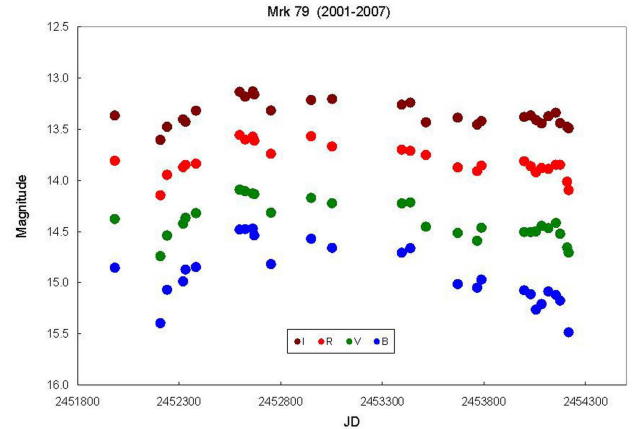


FIG. 6.— The light curves for Mrk 79.

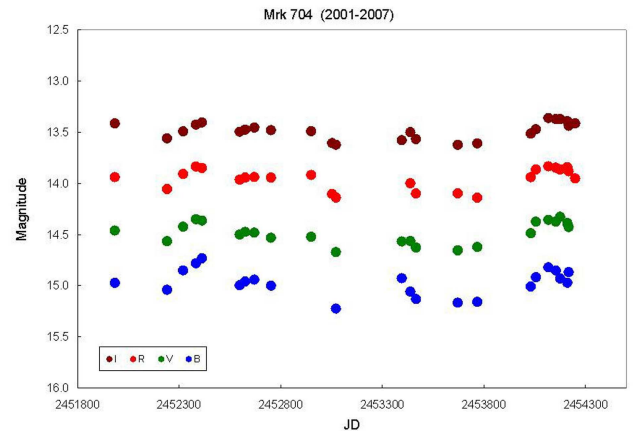


FIG. 7.— The light curves for Mrk 704.

5. CONCLUSION

Although we are not yet ready to begin working on reverberation mapping for 3C-120, Mrk 79, and Mrk 704, we have determined magnitudes for comparison stars that are internally consistent and assembled light curves using data from 2001 March 15 through 2007 May 28.

This project was funded by a partnership between the National Science Foundation (NSF AST-0552798), Research Experiences for Undergraduates (REU), and the Department of Defense (DoD) ASSURE (Awards to Stimulate and Support Undergraduate Research Experiences) programs.

REFERENCES

- de Vaucoulerus, G.A., et al. *Third Reference Catalogue of Bright Galaxies*. New York: Springer; 1991.
- Landolt, Arlo U. 1992, *Astronomical Journal*, 104, 340-371.
- Peterson, B.M. 2007, *An Introduction to Active Galactic Nuclei*. Cambridge University Press, 1-5, 8, 82-7.
- Peterson, B.M. 2004, *The Broad-Line Region in Active Galactic Nuclei*, 1, 4-7.